Supplemental Digital Content 1

Mechanical power and the development of Ventilator-Induced Lung Injury

Massimo Cressoni, Miriam Gotti, Chiara Chiurazzi, Dario Massari, Ilaria Algieri, Martina Amini, Antonio Cammaroto, Matteo Brioni, Klodiana Nikolla, Mariateresa Guanziroli, Daniele Dondossola, Stefano Gatti, Vincenza Valerio, Paola Pugni, Paolo Cadringher, Nicoletta Gagliano, Luciano Gattinoni

TABLE OF CONTENTS

Study protocol – additional methods

Anesthesia was induced with an intramuscular injection of medetomidine 0.025 mg/kg and tiletamine/zolazepam 5 mg/kg. Thereafter, we cannulated an auricular vein. Keeping the animal prone, after pre-oxygenation, we inserted an endotracheal tube (internal diameter 6 mm) and started mechanical ventilation. During surgical preparation, mechanical ventilation was set in volume-controlled mode (FiO_2 0.5, Tidal Volume (V_T) 10 ml/kg, respiratory rate 20-22 breaths/min in order to obtain physiological $EtCO_2$, Inspiratory : Expiratory ratio (I:E) 1:2, no post-inspiratory pause and positive end-expiratory pressure (PEEP) 3-5 cmH_2O.

Anesthesia was maintained with propofol 5-10 mg/kg/h, pancuronium bromide 0.3-0.5 mg/kg/h and midazolam 0.25-1 mg/kg/h. Normal saline (NaCl 0.9%) was administered at 100 ml/h during surgery, then 50 ml/h. Ceftriaxone 1 g i.v. and Tramadol 50 mg i.v. were administered preoperatively, and every 12 hours during the study protocol. Low molecular weight heparin 1900 IU s.c. was administered every 12 hours, after surgery. The animal was turned supine for surgical preparation, carried out under sterile conditions, with piglet under general anesthesia. Right carotid artery was exposed and cannulated. A three lumen central venous catheter was inserted through the right internal jugular vein. A bladder catheter was positioned via cistostomy. At the end of surgery, the animal was turned prone. After performing gastric suction, a latex thin wall, 5 cm long, esophageal balloon was advanced in the inferior third of the esophagus and filled-in with 1.5 ml of room air. Proper positioning of esophageal balloon and endovascular catheters was later verified on thorax computed tomography (CT). Pressure transducers were connected to the endotracheal tube, the esophageal balloon and the endovascular catheters, zeroed at room air at heart level, as appropriate. Esophageal balloon position was checked with CT scan.

Hemodynamic protocol

To maintain hemodynamic stability, a target mean arterial pressure (MAP) was set between 60 and 90 mmHg, with continuous saline infusion (50 ml/h). A fall in MAP below 60 mmHg was corrected with 100-250 ml saline bolus and increases in saline infusion, up to 75-100 ml/h. If these were not sufficient to restore the target MAP, norepinephrine (0.1-1.0 μg/kg/min) was administered. If MAP rose above 90 mmHg, hemodynamic support was deescalated. Cumulative fluid intake was computed as the sum of fluids infused. Drugs were not included. Fluid balance was computed as cumulative fluid intake minus total urinary output.

Data collection and computation

A complete data collection was performed every 6 hours. If respiratory mechanics or hemodynamic variables changed (i.e. increase in peak/plateau pressure despite tracheal suctioning, decrease in peripheral saturation, unexpected arterial hypotension or hypertension), data were also collected. Prior to data collection and, in particular, before respiratory mechanics measurements, tracheal suctioning was performed. V_T, airways pressure and esophageal pressure were recorded during tidal ventilation and during end-inspiratory and end-expiratory pauses.

Transpulmonary pressure was computed at end-inspiration as:

- Transpulmonary pressure (cmH_2O) = ΔAirway pressure (cmH_2O) – ΔEsophageal pressure (cmH_2O)

Where:

- ΔAirway pressure (cmH_2O) = Plateau airway pressure (cmH_2O) – End expiratory pause airway pressure (cmH_2O)

- ΔEsophageal pressure (cmH_2O) = Plateau esophageal pressure (cmH_2O) – End expiratory pause esophageal pressure (cmH_2O)

Plateau airway and esophageal pressures were measured during a 5 seconds end-inspiratory pause.

Respiratory system (E_{RS}), lung (E_L) and chest wall (E_{CW}) elastance were calculated as:

- E_{RS} = ΔAirway pressure (cmH_2O) /V_T

- E_L = (ΔAirway pressure (cmH_2O) – ΔEsophageal pressure (cmH_2O)/V_T
  = Δ Transpulmonary pressure (cmH_2O)/V_T

- E_{CW} = ΔEsophageal pressure (cmH_2O)/V_T

Arterial and central venous blood gases were analyzed (ABL825FLEX, Radiometer, Copenhagen, Denmark®). Central venous pressure was measured during an end-expiratory pause. Internal body temperature was measured. Elevations in body temperature (over 40.0 °C) were managed with acetaminophen (15 mg/kg) and/or physical methods (ice in correspondence of femoral and axillary arteries).

Data collection was completed with performance of 2 CT scans: the former was obtained during an end-inspiratory pause, the latter during an end-expiratory pause.

Sacrifice and autopsy

After the scheduled 54 hours of the study, or before if whole lung edema developed, piglets were sacrificed with a bolus injection of KCl 40 mEq i.v. under deep sedation (50 mg bolus dose of propofol). After sacrifice, autopsy was performed. Chest was opened and lungs along with tracheobronchial tree were excised and weighed.

Light microscopy

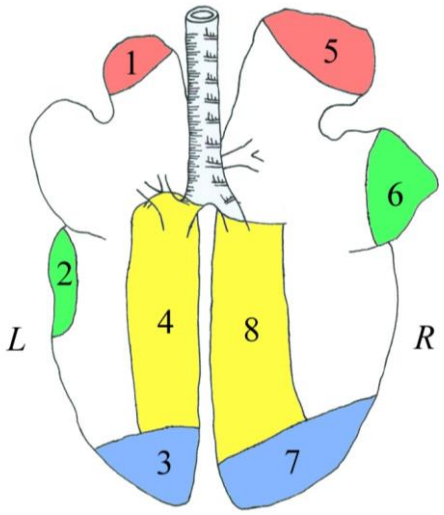

Figure 1: Histology. The colored areas represents the lung regions where lung fragments were collected for histological analysis. Lung fragments for histological analysis were obtained from regions from 1 to 8. Three samples from subpleural regions taken at the tips of the lobes (regions 1, 2, 3, 5, 6, 7) and one sample from the internal part of the lung (regions 4 and 8).

Four regions in each lung were considered, as shown in Figure 1. Fragments were immediately processed for morphological procedures by fixation in 4% formalin in 0.1 M phosphate buffered saline (PBS), pH 7.4. After fixation lung fragments were routinely dehydrated, paraffin embedded, and serially cut (thickness 5 μm). For each specimen and for each staining we analysed three slides obtained at a 100 μm distance. Sections were stained with freshly made haematoxylin-eosin to evaluate cells and tissue morphology. Haematoxylin-eosin stained sections for each lung region were analysed at light microscope in blind by two independent operators using a semi-quantitative grading scale to assess various features of the tissue. The variables included in the scale for the analysis of lung structure and damage were: hyaline membranes formation, diffusion and severity of interstitial and septal infiltrate, vascular congestion and intra-alveolar haemorrhaging, alveoli rupturing and basophilic material deposition. Overall injury was expressed by a scoring system from 0 to 4: 0) no alterations, 1) 25% of field involved; 2) 50 % of field involved; 3) 75 % of field involved; 4) 50-100% of field involved.

Wet to dry ratio

Three samples from each lung (~ 1 cm^3) were collected (upper, medium and lower lobe respectively). They were immediately weighed and, after being dried for 24 hours at 50 °C, were weighed again. Wet to dry ratio, that is an indicator of lung edema, was determined as the ratio between the two measurements.

Lung Computed Tomography

Lung CT scans (Lightspeed, General Electric) were performed with the following settings:

- Collimation width: 32 x 2 x 0.6 mm
- Spiral pitch factor: 1.2
- Slice thickness: 5 mm
- Reconstruction interval: 5 mm
- Data collection FOV: 500 mm
- Reconstruction FOV: 300 mm
- KVp: 120
- X-Ray Tube Corrent: 110 mA
- Pixel dimensions: 0.585938/0.585938
- Acquisition matrix: 512 x 512

Quantitative analysis of CT scan

Lung profiles were manually drawn on each CT scan. Analysis was performed using a dedicated software (SoftEFilm, Elekton, Italy), assuming the density of lung parenchyma to be close to the density of water (0 HU). Each voxel can be analyzed assuming that it is made of two compartments: air (-1000 HU) and lung tissue (including blood, 0 HU).

For each voxel, gas fraction was computed as follows:

Volume gas / (volume gas + volume tissue) = mean CT number observed / (CT number gas – CT number tissue)

Rearranging:

Gas fraction = voxel density (Hounsfield units) / -1000

Tissue fraction = 1 – gas fraction

Consequently, gas and tissue volumes were defined as:

Gas volume = gas fraction x voxel volume

Tissue volume = tissue fraction x voxel volume

Voxel weight is equal to the tissue volume, assuming that tissue density is 1.

Aeration of lung parenchyma was classified in four subsets:

- Not inflated tissue: density > -100 HU
- Poorly inflated tissue: -500 HU < density < -100 HU
- Well inflated tissue: -900 HU < density < -500 HU
- Over inflated tissue: density < -900 HU

We defined "new densities" discrete regions of at least 6 mm (inner diameter of tracheal tube) of maximal diameter with a density corresponding to poorly or not inflated tissue, not present in the previous CT scan and distinguishable from the surrounding parenchyma. [2] We visually classified the CT scan damage as follows:

- Grade 0: baseline CT scan.
- Grade 1: new densities clearly distinguishable from the surrounding parenchyma.
- Grade 2: density occupying at least 1 lung field (apex-hilum-base and dependent/non dependent).
- Grade 3: density occupying all the 6 lung fields (whole lung edema).

Piglet lung acinus size determination for inhomogeneity analysis

As the ratio between airway space dimensions and animal weight follows a logarithmic scale we estimated the acinar volume of piglets from the data presented by Sapoval and Weibel [3] reporting the acinus size in mouse, rat, rabbit and humans. For humans we used the 1/8 subacinus since, as detailed by the authors, this 1/8 subacinus is more comparable to acini in other species and computed an acinar volume of 12.1 mm^3 corresponding to a radius of 1.42 mm.

Lung inhomogeneities determination[4]

CT scan images are composed by voxels whose dimensions depend both on the CT scan hardware and on the setting for image reconstruction. We produced a lung inhomogeneities map with dimensions 1:1 to the original CT scan map, but using as a "basic dimension" the acinar volume and filtering the map with a gaussian filter with a radius equal to the radius of the acinus. We obtained a CT value of each voxel which was dependent to the CT value of the neighboring voxels. Around each voxel we defined a spherical crust starting at distance of one acinar radius from the voxel center and of ½ acinar radius thickness. The ratio of the surrounding voxel gas to the central voxel gas fraction indicates homogeneity if equal to 1, inhomogeneity when greater than 1. We computed a vector of lung inhomogeneities dividing the filtered gas fraction in each of the voxels included, at least partially, in the spherical crust, and the filtered value of the central voxel and we wrote the maximum of the vector in the lung inhomogeneities map. While average is a square filter and takes into the same account near and far voxels, gaussian filters exponentially decreases weight of far voxels. We considered as stress raisers those points causing inhomogeneities greater than 95^{th} percentile of the values observed in our normal piglets at baseline, resulting in a threshold of 1.685. Lung inhomogeneity can be expressed as intensity (average ratio) and extent (fraction of lung volume with inhomogeneities 1.685).

Energy computations per breath

Mechanical power = energy per breath times respiratory rate

The delivered energy per breath (airways + lung) was defined as the area between the inspiratory limb of the Δ-transpulmonary pressure (x) – volume curve and the volume axis (y) and was measured in Joule (filled area in Figure 2 here below).

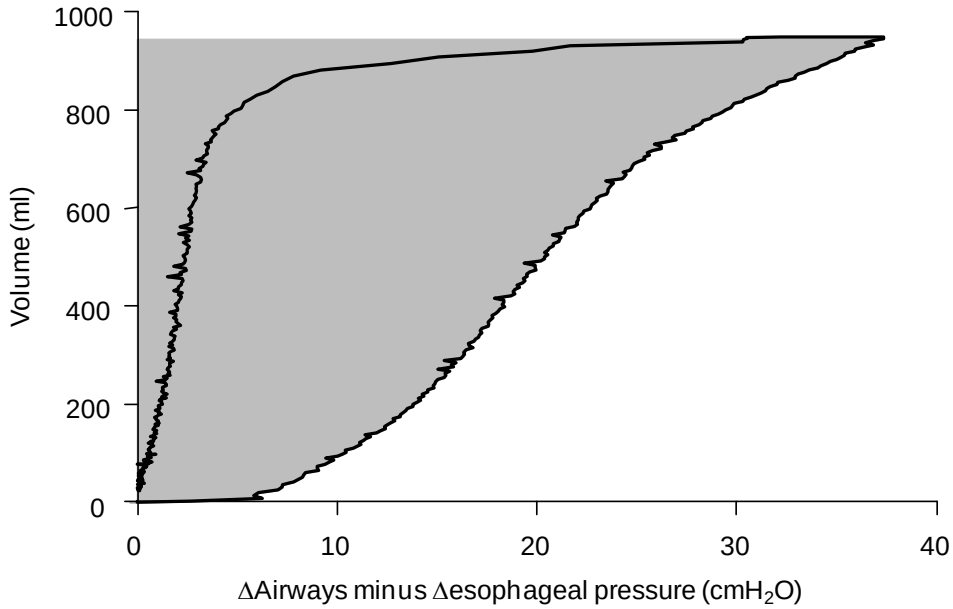

Figure 2: **Dynamic (tidal breath) transpulmonary pressure-volume curve**. An example of dynamic pressure-volume curve (V_T 750 ml, RR 6 bpm, I:E 1:2, no post-inspiratory pause).

Energy was computed on the pressure-volume graph:

Energy (N*m) = Pressure (N/m^2) * Volume (m^3)

To convert cmH_2O*ml in Joule:

1 J = 1 Pa * m^3

1 Pa = 0.0101971621298 cmH_2O

1 m^3 = 1000000 ml

1 J = 0.0101971621298 cmH_2O * 1000000 ml = 10197.16 cmH_2O * ml

1 cmH_2O * ml = 0.0000980665 J

Relationship between total delivered energy to the respiratory system components

In order to analyze the relationships between the different components in which energy is spent during tidal ventilation (see Figure 3), we performed additional measurements in six piglets. Before the beginning of the study (i.e. when all animals' lungs were still healthy), dynamic (i.e. during tidal ventilation) and static pressure-volume curves were acquired at different combinations of V_T and RR. In the same animals, after autopsy, the same V_T-RR combinations were used to acquire pressure-volume curves on the isolated endotracheal tube/tracheobronchial tree. Below we reported the combinations:

1) Dynamic pressure-volume curves, obtained during tidal ventilation:
   - RR 15 breaths/min (I:E 1:2) and V_T 150-300-450-600-750-900 ml, no post-inspiratory pause
   - V_T 450 ml and RR 3-6-9-12-15 breaths/min (I:E 1:2), no post-inspiratory pause.
2) Static pressure-volume curves, obtained with a super-syringe, as previously described:
   - V_T 150-300-450-600-750-900 ml
3) Airways pressure-volume curves, obtained during tidal ventilation of the endotracheal tube/tracheobronchial tree as previously described:
   - RR 3-6-9-12-15 breaths/min (I:E 1:2) and V_T 150-300-450-600-750-900 ml: each possible combination)

Energy delivered per breath to the respiratory system can be divided into different components which are detailed in Figure 3. A detailed explanation of where energy is spent during mechanical ventilation is relevant, as only the energy dissipated within the lung parenchyma may contribute to Ventilator-Induced Lung Injury while the energy dissipated outside the lung should not contribute to VILI. The use of esophageal pressure (see Figure 4) allows to remove the chest wall component. We left the energy dissipated into the airways in the main text definition of mechanical power but estimated the quota spent to overcome endotracheal tube and trachea (Figure 5-6 and 8). Figure 12-13-14 demonstrate the dependency of all energy quotas on both flow and tidal volume. Figure 16 and 17 show that all the energies per breath we computed are related each other and that our results would have been similar if a different definition of energy would have been used.

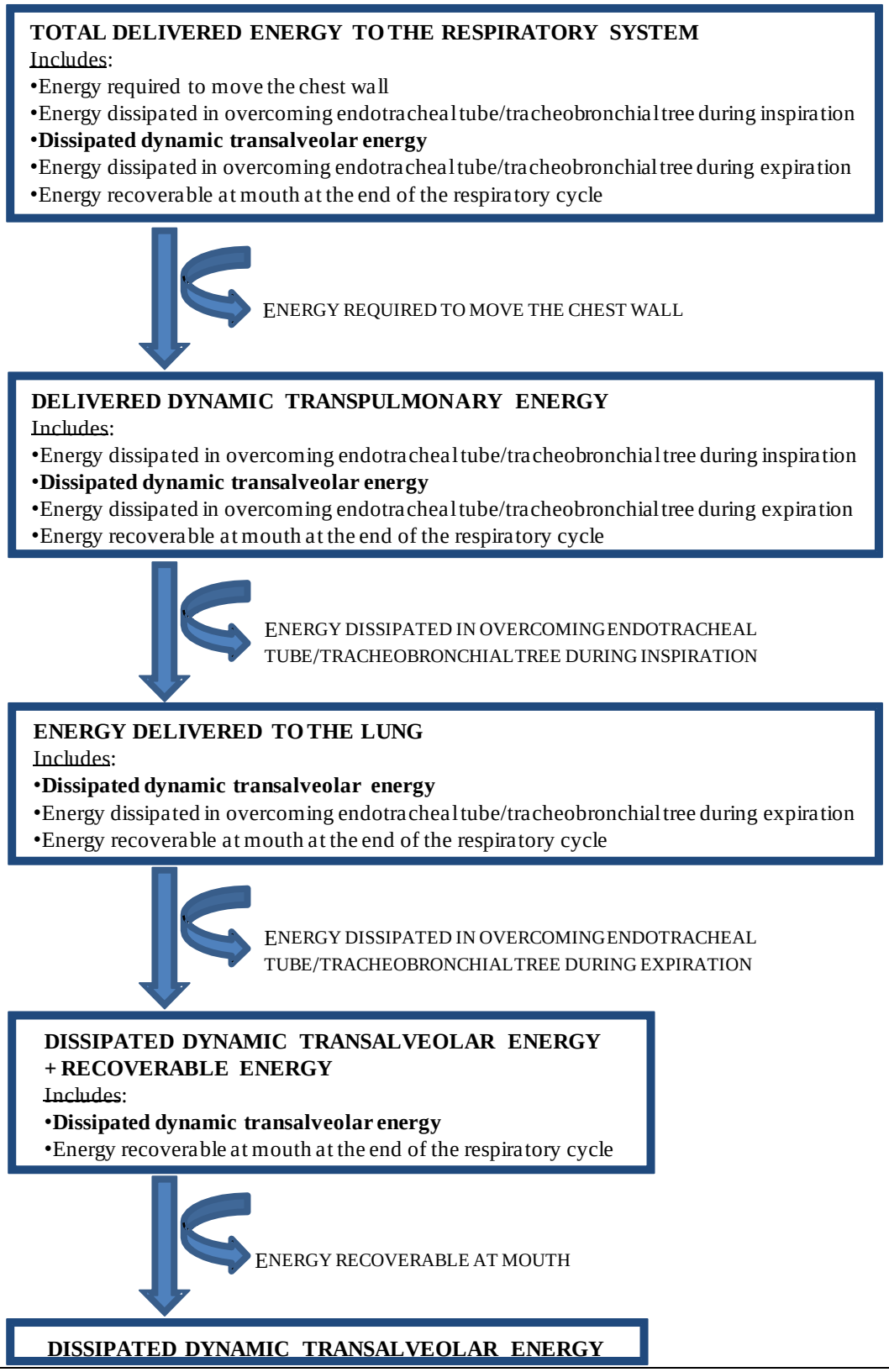

Figure 3: Definitions of components of total delivered energy to the respiratory system. In our hypothesis, when the dissipated dynamic transalveolar energy overcomes the threshold, VILI occurs.

Remove energy spent to move chest wall

To obtain the delivered dynamic transpulmonary energy (i.e. remove chest wall component):

1. Esophageal pressure was filtered to eliminate the cardiac beat artifact (Figure 4, Panel A, indicated with red line).
2. Filtered esophageal pressure trace was subtracted from the airways pressure trace (Figure 4, Panel B), obtaining an airways *minus* esophageal pressure trace (Figure 4, Panel C).
3. The pressure-volume curve was plotted, using the airways-esophageal pressure trace, starting from the origin of the axis (zeroed).
4. The transpulmonary energies were computed as the area between the inspiratory limb of the pressure-volume curve and the volume axis (see Figure 2).

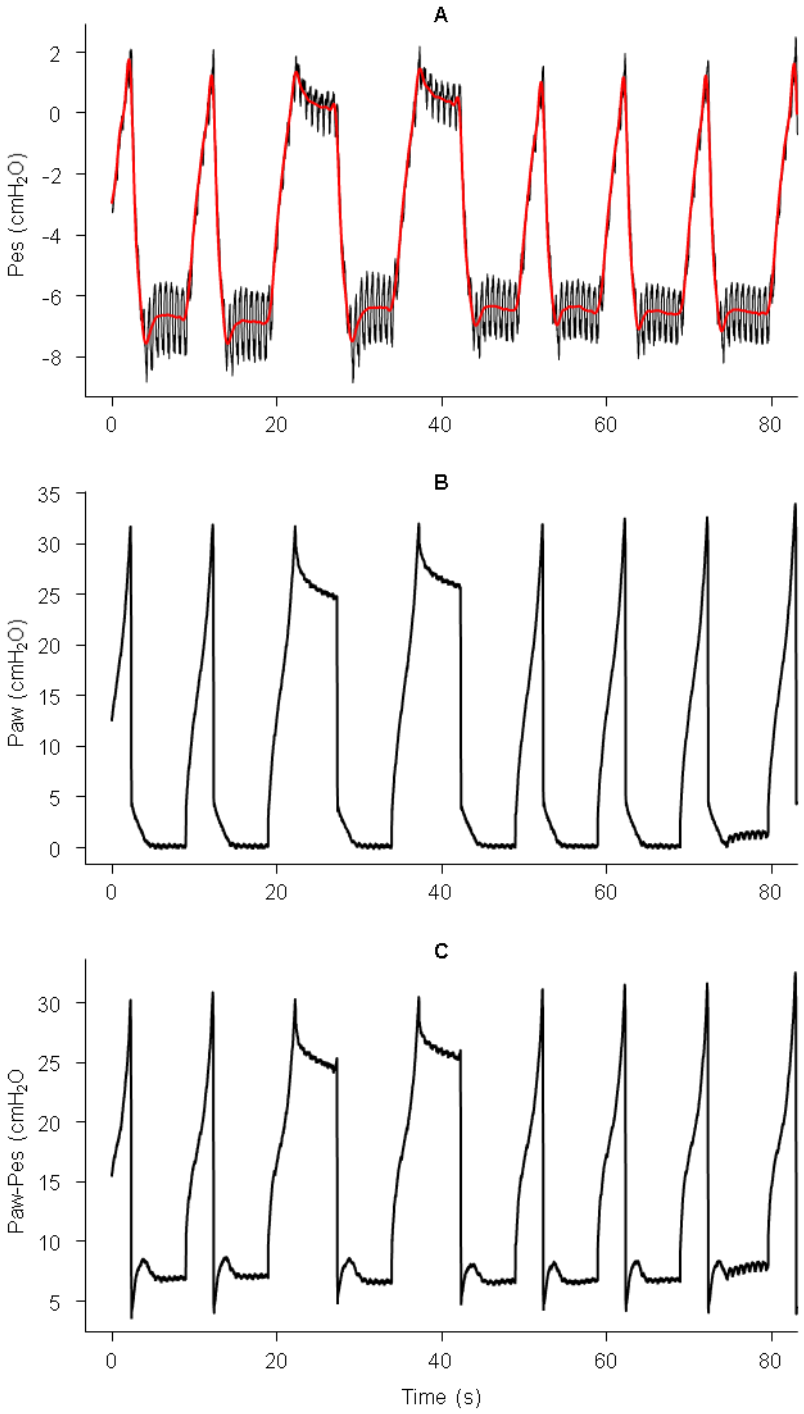

Figure 4: steps to obtain airways minus esophageal pressure trace. An example of filtering esophageal pressure (Panel A), and subtraction from the airways pressure (Panel B) the filtered esophageal pressure obtaining the airways minus esophageal pressure trace (Panel C). Of note, subtraction does not represent transpulmonary pressure, since absolute esophageal pressure is not pleural pressure. However, the changes in esophageal pressure correspond to the changes in pleural pressure.

Airways dissipated energy during inspiration – *ex-vivo setting*

Lung parenchyma and blood vessels were manually removed in order to isolate the tracheobronchial tree. An endotracheal tube (same internal diameter used during the experiment) was positioned and connected to the filter (Covidien DAR^{TM} Adult – Pediatric Electrostatic Filter HME Small) and breathing circuit (Covidien PVC Smoothbore Breathing System, 100 cm), as during experiment (Figure 5). Colligo (www.elekton.it) was connected between filter and breathing circuit, as during experiment to measure pressure and flow.

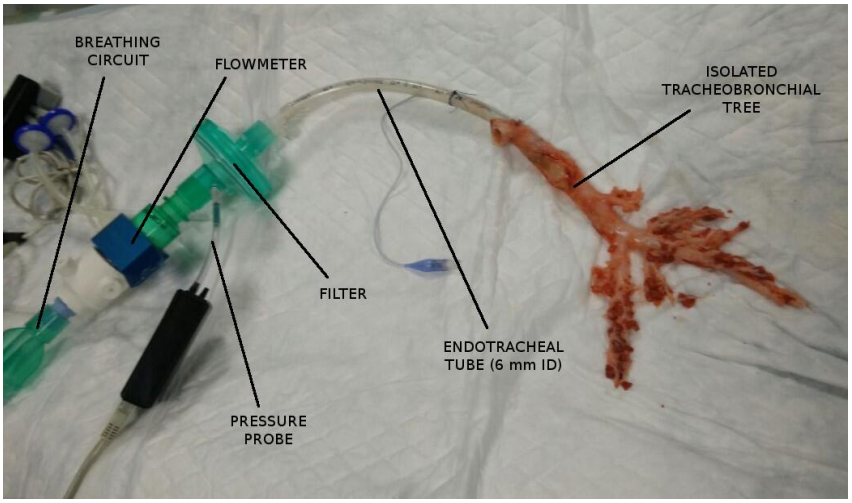

Figure 5: Determination of airways pressure-volume curve. *Ex* vivo model to quantify energy dissipated in overcoming airway resistances during inspiration.

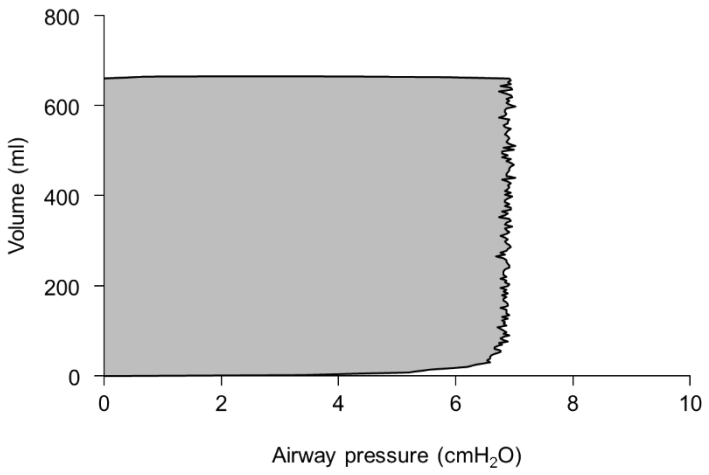

Figure 6: Airways pressure-volume curve. An example of airways pressure-volume curve (V_T 600 ml; RR 12 bpm; I:E 1:2, no post-inspiratory pause). The filled area represents the energy dissipated into endotracheal tube/tracheobronchial tree during inspiration.

Energy dissipated in overcoming endotracheal tube/tracheobronchial tree resistances during expiration

Energy dissipated in overcoming airway resistances during expiration is function of V_T (ml/kg) and expiratory flow (ml/kg/s). Expiratory flow was computed as average flow:

- Expiratory flow (ml/kg/s) = V_T (ml/kg) / expiratory time (s)

Actually, expiratory time must be intended as time needed for complete expiration. This does not necessarily correspond to expiratory time as set on the ventilator (i.e. (60 s / RR) * (1 – I:E)).

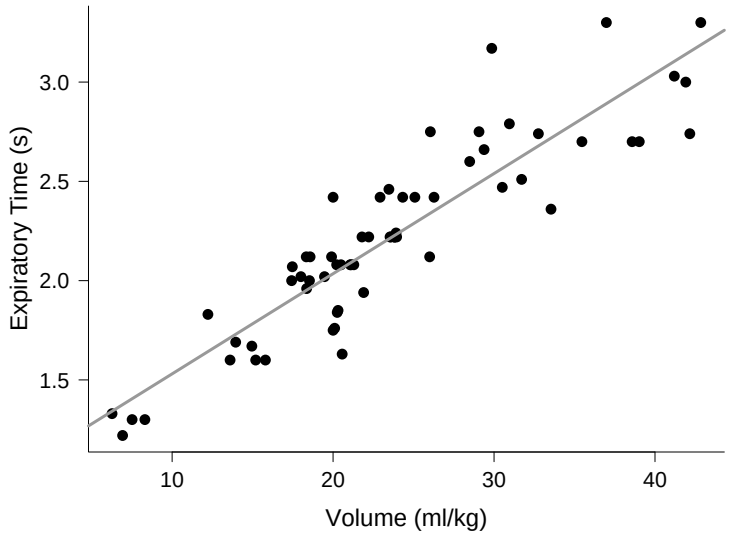

Figure 7: Time needed to complete expiration as function of V_T. Being expiration a passive process, expiratory time is only function of V_T. Expiratory time (s) = 1.026 + 0.050* V_T (ml/kg), r^2=0.82, p<0.0001.

Assuming, as an approximation, that airway resistances are similar both during inspiration and expiration, the effect of expiratory flow on energy dissipation would be similar to that of inspiratory flow. Therefore, we can derive the energy dissipated into endotracheal tube/tracheobronchial tree during expiration from the equations of the airways (see Figure 8) considering expiratory flow instead of inspiratory flow.

Energy recoverable at mouth during tidal ventilation

The energy recoverable at mouth during tidal ventilation corresponds to the amount of energy which is not dissipated into the respiratory system at the end of expiration; this energy, theoretically, could be recovered at mouth, connecting to the endotracheal tube an appropriate device to collect energy. This component is specific of our model, and is measurable as the area between the expiratory limb of the pressure-volume curve and the volume axis (y).

Static dissipated energy into the respiratory system

To obtain the static airways pressure-volume curve graph, after pre-oxygenation, inflation and deflation of the lungs were performed with a supersyringe in steps of 100 ml (last step during inflation and first step during deflation of 50 ml, if necessary) every ~ 3 seconds. Deflation was interrupted when resistance was encountered (Figure 8 – dashed curve). Static dissipated energy into the respiratory system is the hysteresis area of the airways pressure-volume curve.

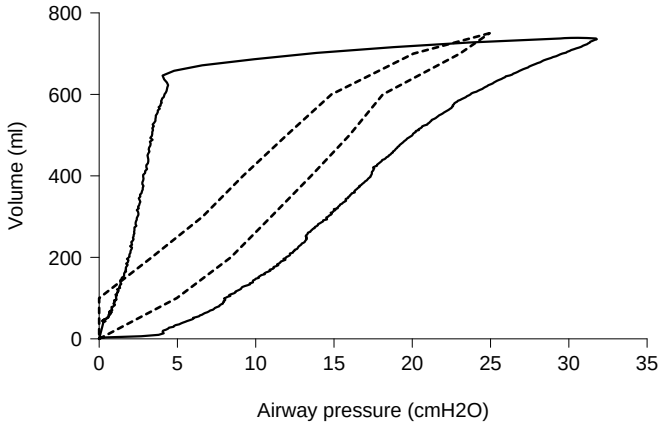

Figure 8: static and dynamic airways pressure-volume curve. For the same volume (750 ml), dynamic hysteresis area (solid line), recording during tidal ventilation at respiratory rate 6 breaths/min and I:E = 1:2, is greater that static hysteresis area (dashed line) because of flow-dependent phenomena (airways dissipation energy and flow dependent component of dissipated dynamic trans-alveolar energy).

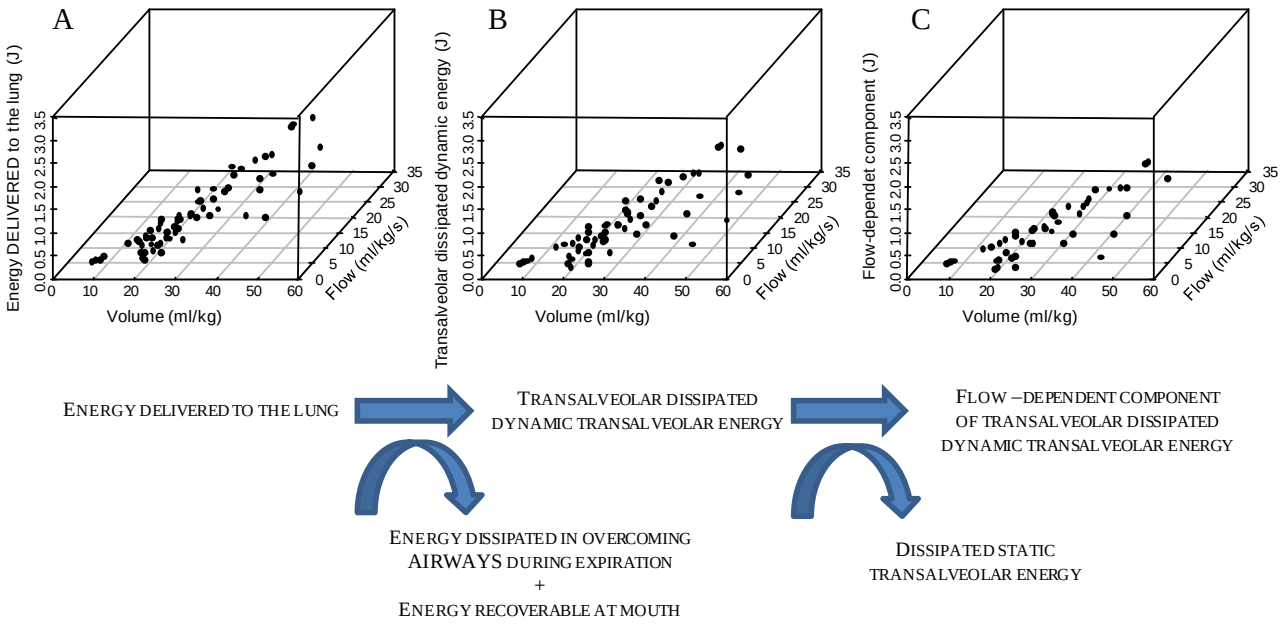

Figure 9: Sequential calculation of dissipated dynamic transalveolar (TA) energy (B), and flow-dependent component of dissipated dynamic TA energy (C) from the energy delivered to the lung.

We realized this figure subtracting point by point for each piglet:

→ to obtain Panel B from Panel A, its own energy dissipated in overcoming endotracheal tube/tracheobronchial resistances + energy recoverable at mouth (matching tidal volume and respiratory rate)

→ to obtain Panel C from Panel B, its own dissipated static transalveolar energy (matching tidal volume).

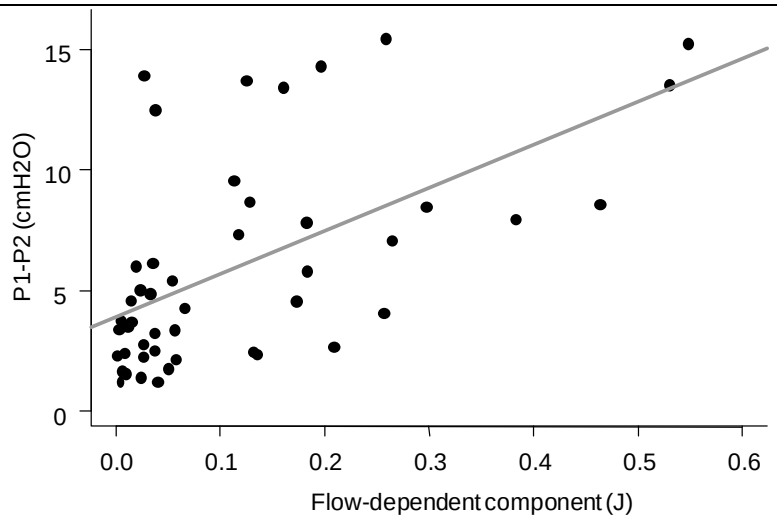

Figure 10: relationship between flow dependent component of dissipated dynamic transalveolar energy and "stress relaxation". On the x axis we reported the energy resulting from the sequential subtraction previously described, including the subtraction from the dissipated dynamic transalveolar energy the static component, computed from the static airways-esophageal pressure-volume curve. On y axis we reported "stress relaxation", quantified as P1-P2 (cmH_2O) during a 5 seconds end-inspiratory pause on the airways pressure – time graph. As shown, there is a linear relationship between "stress relaxation" and the flow dependent component of dissipated dynamic transalveolar energy ($r^2 = 0.34$, $p<0.0001$): (P1-P2) $cmH_2O = 3.9 + 17.9 *$ flow dependent component (J) .

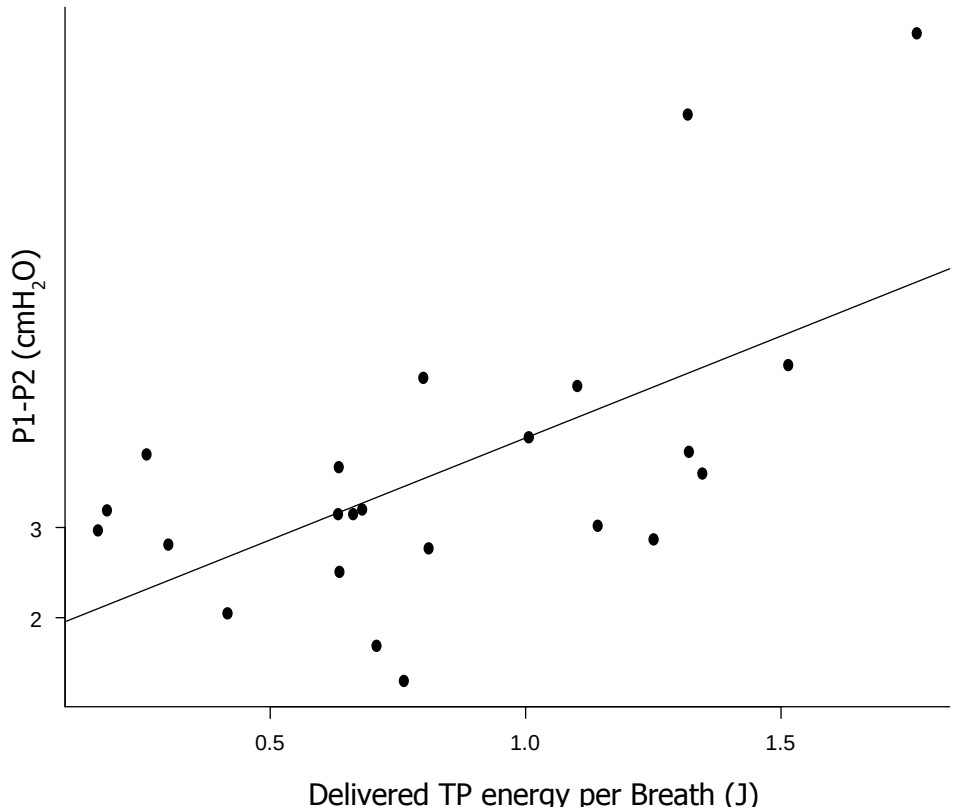

Figure 11: stress relaxation (P1-P2) as function of delivered transpulmonary energy per breath. Data measured at the beginning of the study.
Stress relaxation (P1 – P2, cmH2O) = 2.26*(delivered transpulmonary energy per breath, (J)+ 1.73.

Energy per breath as function of flow and tidal volume

Total delivered energy to the respiratory system

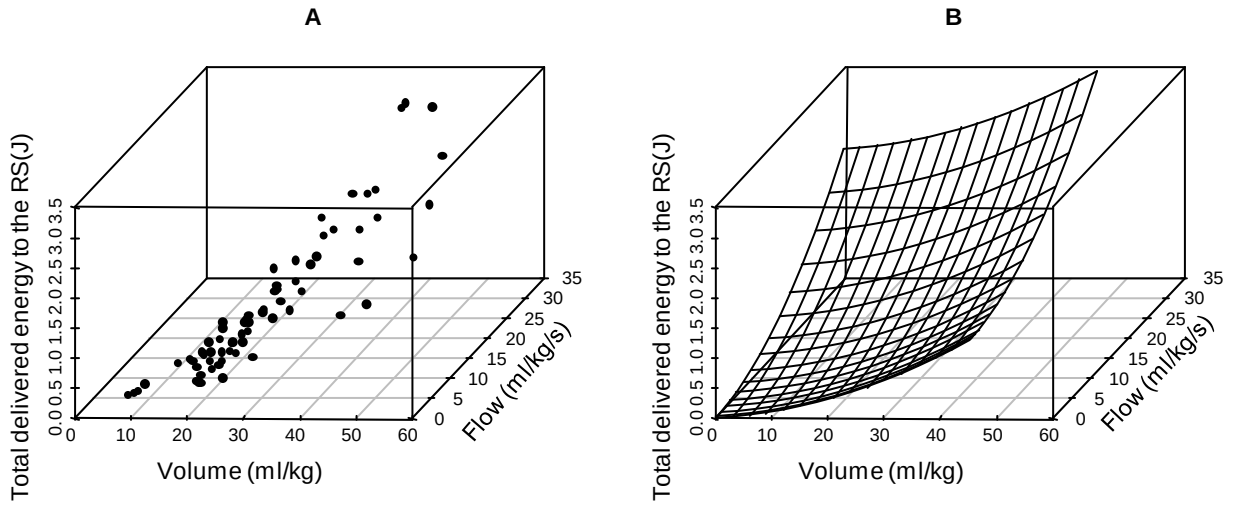

Figure 12: Total delivered energy to the respiratory system at each breath, computed from the dynamic pressure-volume curves, as function of volume and flow. Total delivered energy, computed on the dynamic pressure-volume curves, is function of both V_T and flow (*Panel A*). Data points were fit with a two-variables function (i.e. a surface, shown in *Panel B*) without intercept and with lower constraint 0, obtaining the following equation (r^2=0.92):

(A) Total delivered energy (J) = k1*flow (ml/kg/s)^2 + k2* V_T (ml/kg)^2 + k3* V_T (ml/kg); where:

- k1 = 0.0019033
- k2 = 0.0005165
- k3 = 0.0052903

Delivered dynamic transpulmonary energy

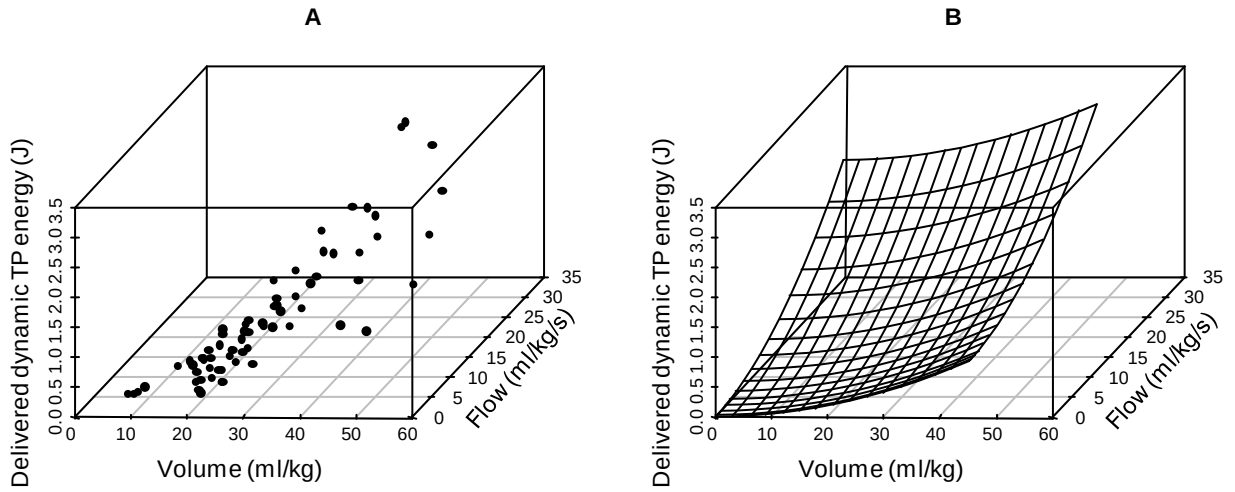

Figure 13: delivered dynamic transpulmonary energy at each breath, computed from the dynamic airways-esophageal pressure-volume curves, as function of volume and flow. Delivered dynamic transpulmonary (TP) energy, computed on the dynamic pressure-volume curves, is function of both V_T and flow (*Panel A*). Data points were fit with a two-variables function (i.e. a surface, shown in *Panel B*) without intercept and with lower constraint 0, obtaining the following equation (r^2=0.87):

(B) Delivered dynamic TP energy (J) = k1*flow (ml/kg/s)^2 + k2* V_T (ml/kg)^2 + k3* V_T (ml/kg); where:

- k1 = 0.0017301
- k2 = 0.0004441
- k3 = 0.0005607

Energy dissipated in overcoming endotracheal tube/tracheobronchial tree resistances during inspiration

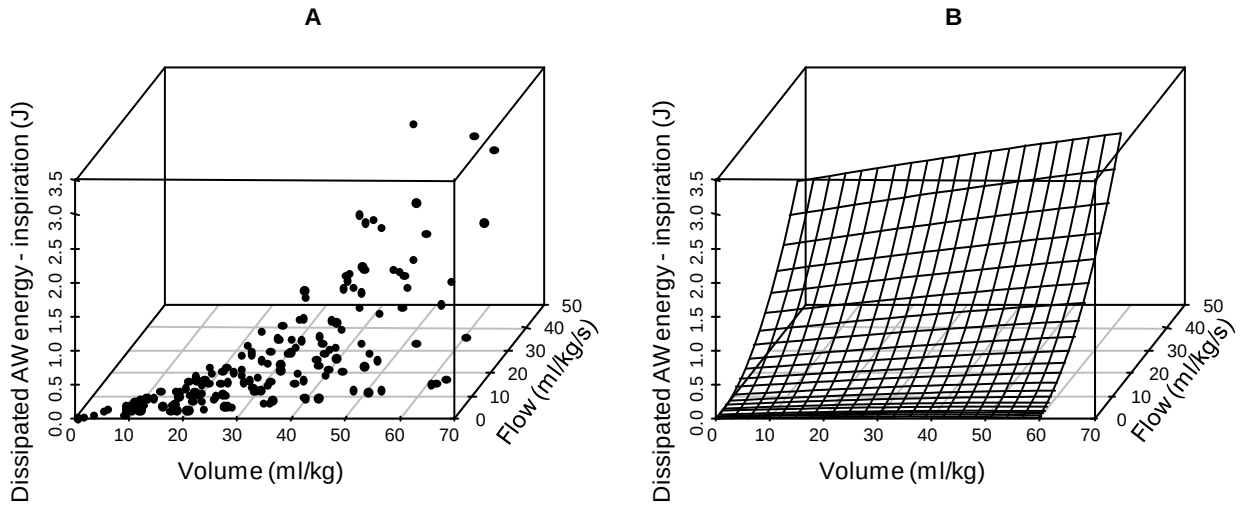

Figure 14: Energy dissipated into endotracheal tube/tracheobronchial tree during inspiration. *Panel A*, energy dissipated into endotracheal tube/tracheobronchial tree (dissipated AW energy) during inspiration is plotted as function of flow and V_T. Energy (J) dissipated in overcoming airway resistances during inspiration is function of V_T (ml/kg) and inspiratory flow (ml/kg/s). Inspiratory flow was computed as average flow:

- Inspiratory time (s) = (60 s / RR) * I:E
- Inspiratory flow (ml/kg/s) = V_T (ml/kg) / inspiratory time (s)

Data points were fit with a two-variables function (i.e. a surface, shown in *Panel B*) without intercept, obtaining the following equation (r^2=0.88, p<0.0001):

(C) Energy dissipated into endotracheal tube/tracheobronchial tree during inspiration

(J) = k1* flow (ml/kg/s)^2 + k2* V_T (ml/kg)^2 + k3* flow (ml/kg/s)* V_T (ml/kg) + k4* flow (ml/kg/s) + k5* V_T (ml/kg); where:

- k1 = $1.121*10^{-3}$
- k2 = $-2.754*10^{-5}$
- k3 = $2.609*10^{-4}$
- k4 = $-7.979*10^{-3}$
- k5 = $1.947*10^{-3}$
- flow = inspiratory flow, as previously computed.

Energy dissipated in overcoming endotracheal tube/tracheobronchial tree with tube of diameter of 6 or 8 mm

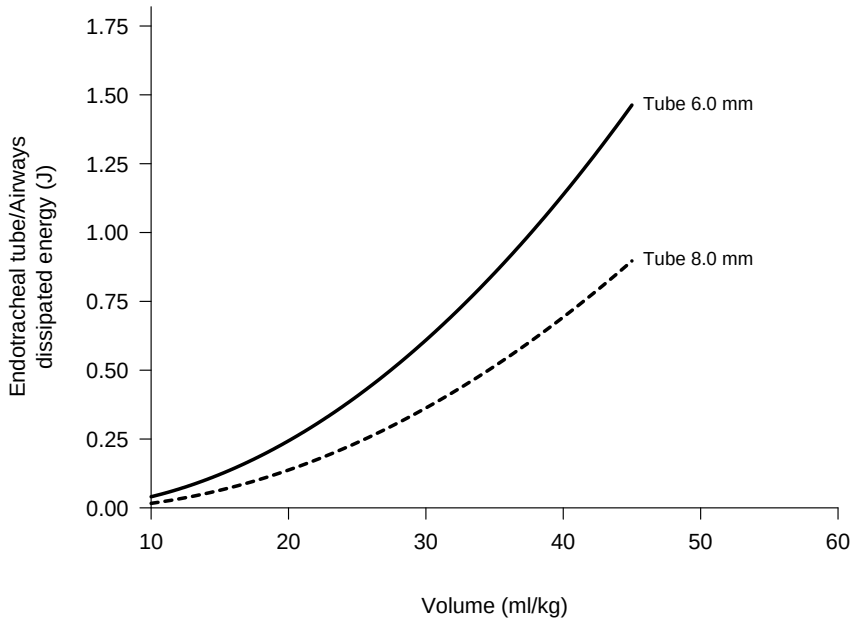

Figure 15: Airways dissipated energy with endotracheal tubes of different diameter. An endotracheal tube with an 8.0 mm internal diameter (dashed line) dissipates 40-45% energy less than a 6.0 mm tube (solid line). This measurement was performed on the tracheobronchial tree preparation at the end of the experiment. The figure reports energy values obtained with a respiratory rate of 15 breaths/min (I:E 1:2).

Relationships between the different energy computations

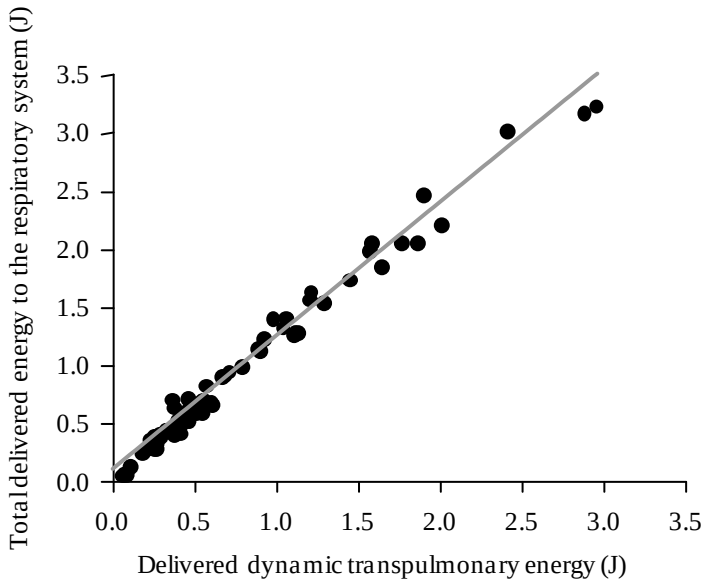

Figure 16: Relationship between total delivered energy to the respiratory system and delivered dynamic transpulmonary energy. In our model, delivered energy to the respiratory system and delivered dynamic transpulmonary energy are strongly related each other (r^2=0.98, p<0.0001):

Total delivered energy to the RS (J) = 0.10146 + 1.14691* Delivered dynamic transpulmonary energy (J)

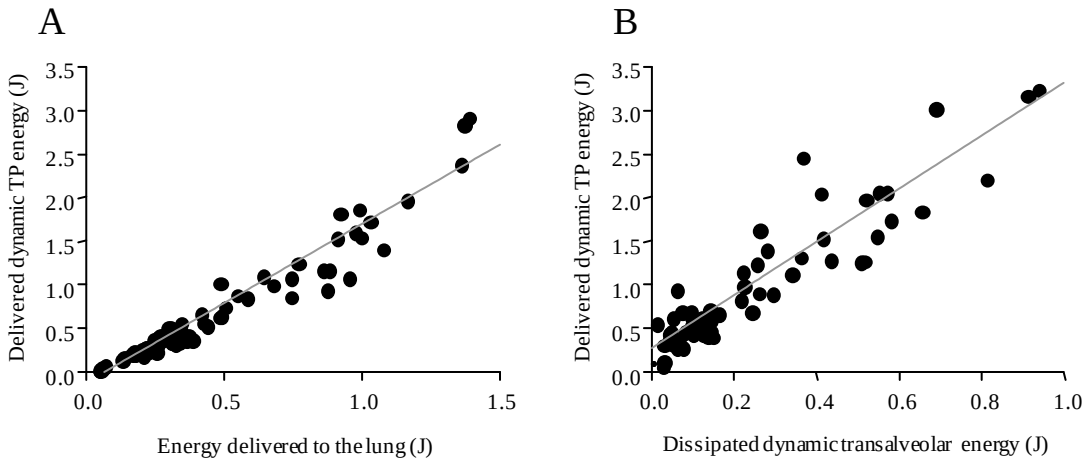

Figure 17: Relationship between delivered dynamic transpulmonary energy and its components. There is a strong linear correlation between delivered dynamic transpulmonary energy and:

- energy delivered to the lung (*Panel A*) (r^2=0.93, p<0.0001):

Delivered dynamic transpulmonary energy (J) = - 0.11787 + 1.80870 * energy delivered to the lung (J)

- dissipated dynamic transalveolar energy (*Panel B*) (r^2=0.86, p<0.0001):

Delivered dynamic transpulmonary energy (J) = 0.27322 + 3.04970 * dissipated dynamic transalveolar energy (J).

Supplementary data from the main experiments

Equations of linear regressions in Table 1 e Table 2 (main text)

In this paragraph we reported equations of linear regressions presented in Table 1 (main text) (Figure 18).

- Weight (kg) = 21.57 – 0.09 * respiratory rate (breaths/min) $r^2 = 0.05$, p=0.44
- Tidal volume (ml) = 796.67 + 0 * respiratory rate (breaths/min) $r^2 = 0.00$, p=1.00
- Tidal volume (ml/kg) = 36.90 + 0.17 * respiratory rate (breaths/min) $r^2 = 0.09$, p=0.27
- Strain = 3.58 – 0.04 * respiratory rate (breaths/min) $r^2 = 0.02$, p=0.64
- Tidal volume/lung tissue (ml/g) = 1.91 + 0.01 * respiratory rate (breaths/min) $r^2 = 0.05$, p=0.48
- Peak pressure (cmH_2O) = 26.50 + 0.89 * respiratory rate (breaths/min) $r^2 = 0.74$, p<0.0001
- Plateau pressure (cmH_2O) = 23.13 + 0.19 * respiratory rate (breaths/min) $r^2 = 0.21$, p=0.09
- Transpulmonary pressure (cmH_2O) = 16.59 + 0.14* respiratory rate (breaths/min) $r^2 = 0.06$, p=0.39
- PaO_2/FiO_2 = 505.53 + 0.44 * respiratory rate (breaths/min) $r^2 = 0.00$, p=0.90
- pH = 7.33 + 0.03 * respiratory rate (breaths/min) $r^2 = 0.64$, p<0.001
- $PaCO_2$ (mmHg) = 55.10 – 2.97 * respiratory rate (breaths/min) $r^2 = 0.61$, p<0.001
- Respiratory system elastance (l/cmH_2O) = 32.75 + 0.03 * respiratory rate (breaths/min) $r^2 = 0.00$, p=0.95
- Lung elastance (l/cmH_2O) = 23.04 + 0.15 * respiratory rate (breaths/min) $r^2 = 0.01$, p=0.67
- Chest wall elastance (l/cmH_2O) = 9.71 – 0.12 * respiratory rate (breaths/min) $r^2 = 0.02$, p=0.60

- Mean arterial pressure (mmHg) = 103.67 – 0.89 * respiratory rate (breaths/min) $r^2 = 0.04$, p=0.47
- Heart rate (beats/min) = 95.23 + 2.19 * respiratory rate (breaths/min) $r^2 = 0.10$, p=0.25
- Total lung volume (ml) = 605.29 + 7.61 * respiratory rate (breaths/min) $r^2 = 0.06$, p=0.43
- Total lung tissue (g) = 415.19 – 2.49 * respiratory rate (breaths/min) $r^2 = 0.09$, p=0.31
- Well inflated tissue (%) = 0.04 + 0.02 * respiratory rate (breaths/min) $r^2 = 0.16$, p=0.17
- Poorly inflated tissue (%) = 0.87 – 0.02 * respiratory rate (breaths/min) $r^2 = 0.21$, p=0.11
- Not inflated tissue (%) = 0.09 – 0.00 * respiratory rate (breaths/min) $r^2 = 0.00$, p=0.96
- Lung inhomogeneity extent (%) = 7.95 + 0.01 * respiratory rate (breaths/min) $r^2 = 0.00$, p=0.94

In this paragraph we reported equations of linear regressions presented in Table 2 (main text) (Figure 18).

- Delivered dynamic transpulmonary energy (per breath) (J)= 0.70 + 0.05 * respiratory rate (breaths/min) $r^2 = 0.35$, p=0.02
- Average inspiratory flow (l/s) = 8.84 + 36.53 * respiratory rate (breaths/min) $r^2 = 0.93$, p<0.0001
- Delivered dynamic transpulmonary energy load (J/min) = -2.69 + 1.51 * respiratory rate (breaths/min) $r^2 = 0.90$, p<0.0001

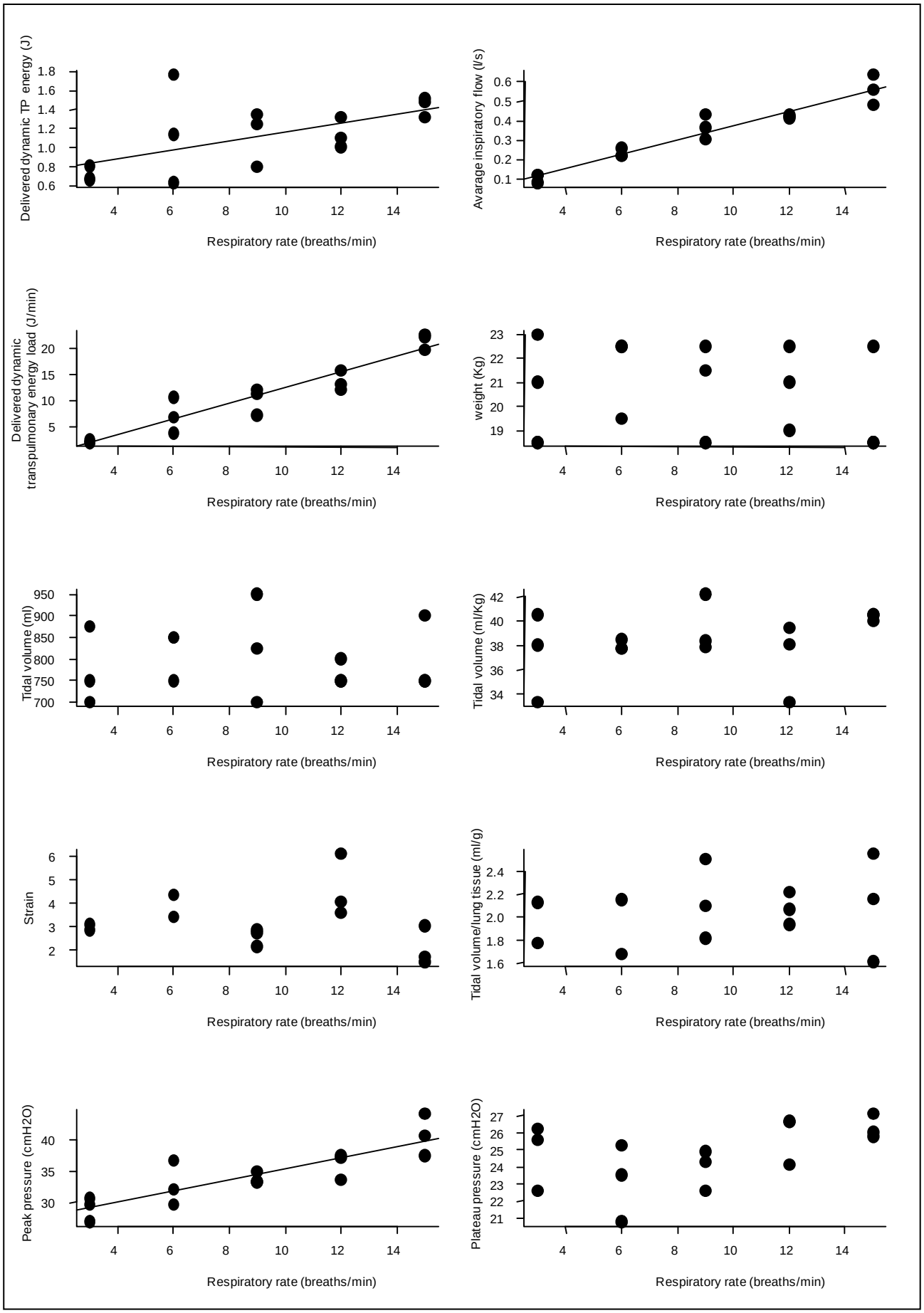
Delivered dynamic TP energy (J)
1.8
1.6
1.4
1.2
1.0
0.8
0.6
4
6
8
10
12
14
Respiratory rate (breaths/min)
Avarage inspiratory flow (l/s)
0.6
0.5
0.4
0.3
0.2
0.1
4
6
8
10
12
14
Respiratory rate (breaths/min)
Delivered dynamic transpulmonary energy load (J/min)
20
15
10
5
4
6
8
10
12
14
Respiratory rate (breaths/min)
weight (Kg)
23
22
21
20
19
4
6
8
10
12
14
Respiratory rate (breaths/min)
Tidal volume (ml)
950
900
850
800
750
700
4
6
8
10
12
14
Respiratory rate (breaths/min)
Tidal volume (ml/Kg)
42
40
38
36
34
4
6
8
10
12
14
Respiratory rate (breaths/min)
Strain
6
5
4
3
2
4
6
8
10
12
14
Respiratory rate (breaths/min)
Tidal volume/lung tissue (ml/g)
2.4
2.2
2.0
1.8
1.6
4
6
8
10
12
14
Respiratory rate (breaths/min)
Peak pressure (cmH2O)
40
35
30
4
6
8
10
12
14
Respiratory rate (breaths/min)
Plateau pressure (cmH2O)
27
26
25
24
23
22
21
4
6
8
10
12
14
Respiratory rate (breaths/min)

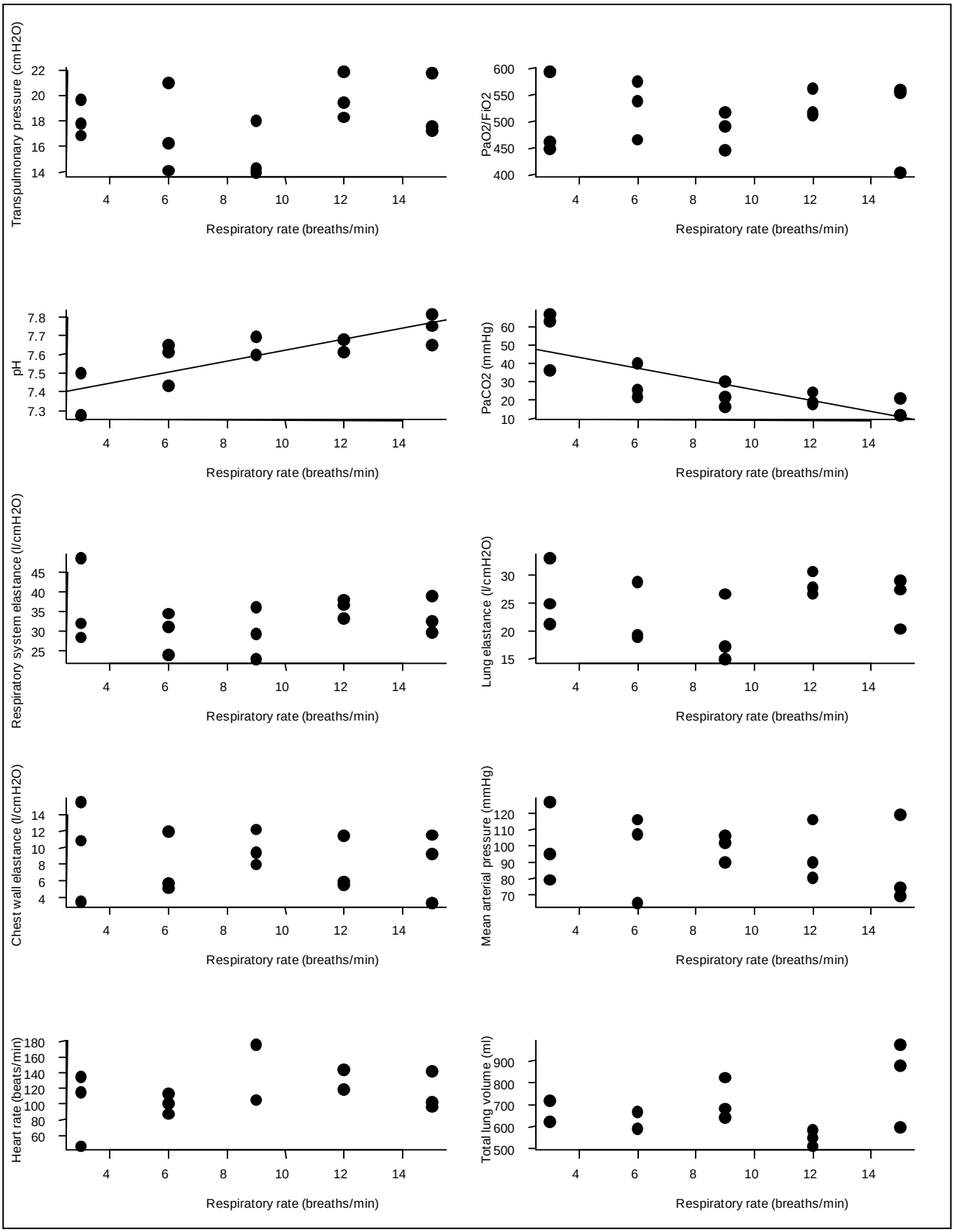
Transpulmonary pressure (cmH2O)
Respiratory rate (breaths/min)
PaO2/FIO2
Respiratory rate (breaths/min)
pH
Respiratory rate (breaths/min)
PaCO2 (mmHg)
Respiratory rate (breaths/min)
Respiratory system elastance (l/cmH2O)
Respiratory rate (breaths/min)
Lung elastance (l/cmH2O)
Respiratory rate (breaths/min)
Chest wall elastance (l/cmH2O)
Respiratory rate (breaths/min)
Mean arterial pressure (mmHg)
Respiratory rate (breaths/min)
Heart rate (beats/min)
Respiratory rate (breaths/min)
Total lung volume (ml)
Respiratory rate (breaths/min)

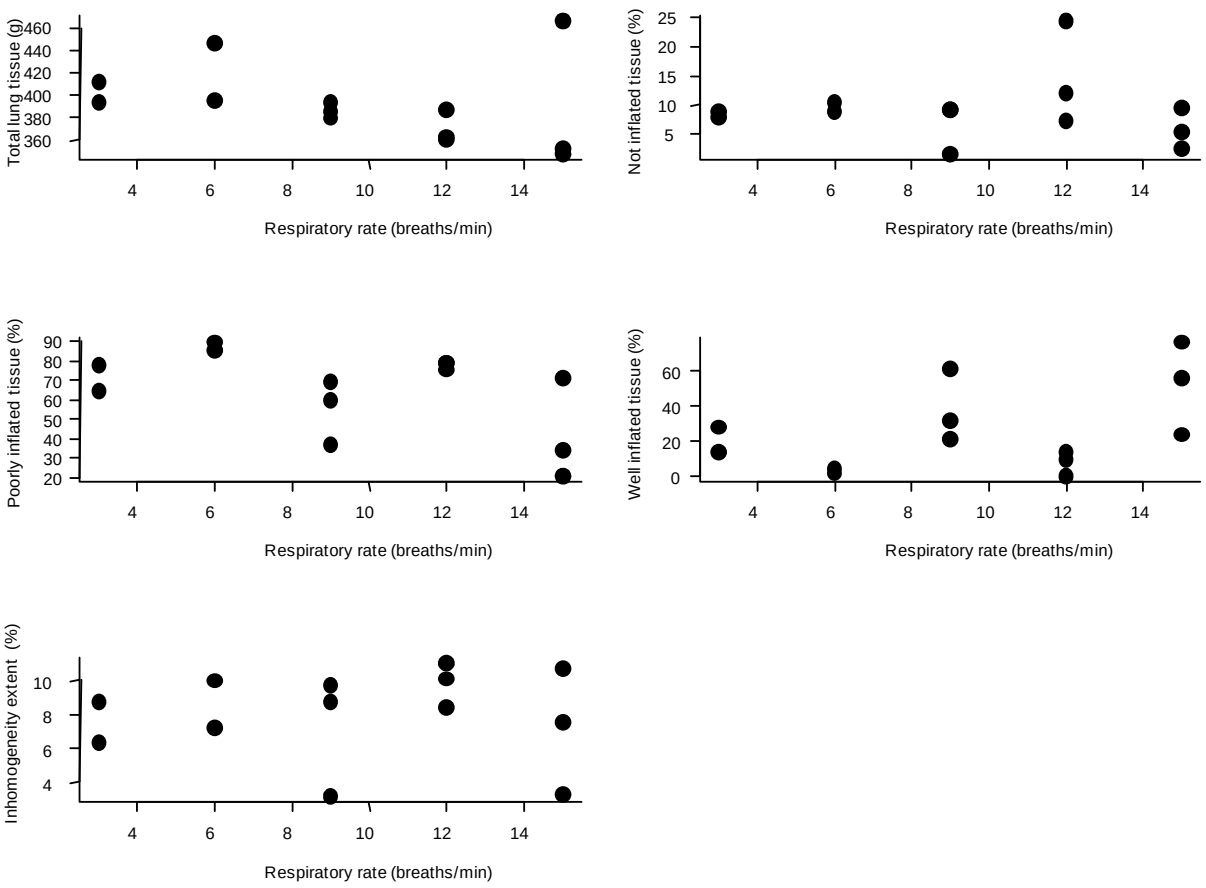

Figure 18: Linear regressions for Table 1 and Table 2 (main text)

Regressions for Figure 4 (main text)

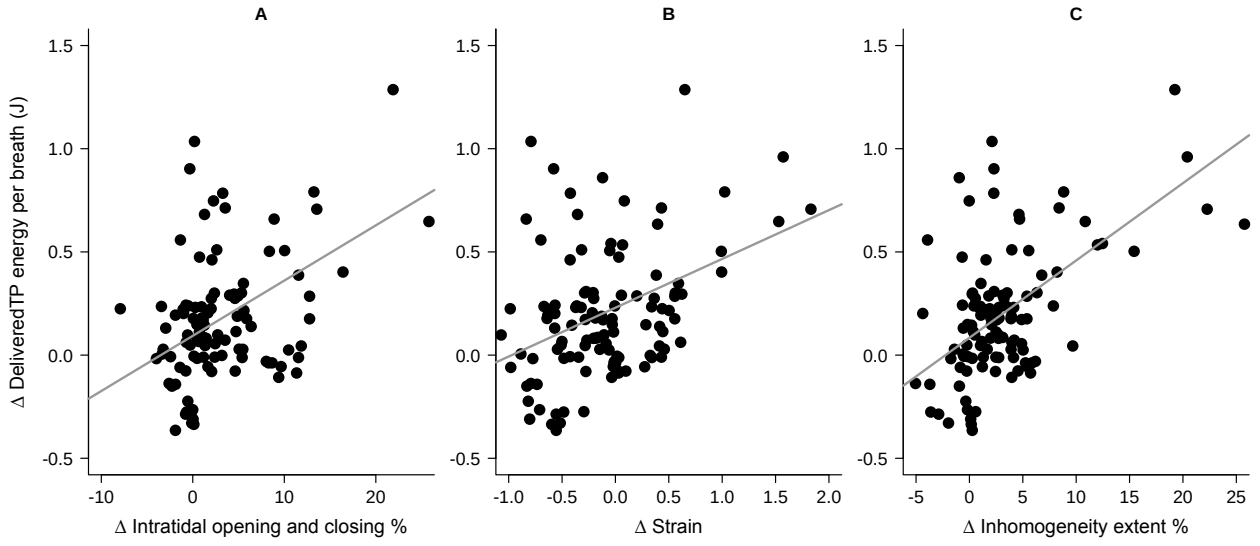

Figure 19: Regressions for Figure 4 (main text). Regressions on the entire pool of data to realize figure 4 (main text). *Panel A*: Δ delivered dynamic transpulmonary energy (J) = 0.09 + 0.03*Δ intratidal opening and closing (%), r^2=0.23, p<0.0001. *Panel B*: Δ delivered dynamic transpulmonary energy (J) = 0.23 + 0.24*Δ strain, r^2=0.14, p<0.0001. *Panel C*: Δ delivered dynamic transpulmonary energy (J) = 0.08 + 0.04*Δ lung inhomogeneity extent (%), r^2=0.37, p<0.0001.

Thresholds calculation

In order to analyze our results, we calculated 3 thresholds of energy load to VILI development (defined as an increase of at least 10% of the lung weight at last CT scan) (Figure 20):

- The first one on total delivered energy load to the respiratory system: 16.7 J/min
- The second one on delivered dynamic transpulmonary energy load: 12.1 J/min
- The third one on delivered energy load to the lung: 6.9 J/min

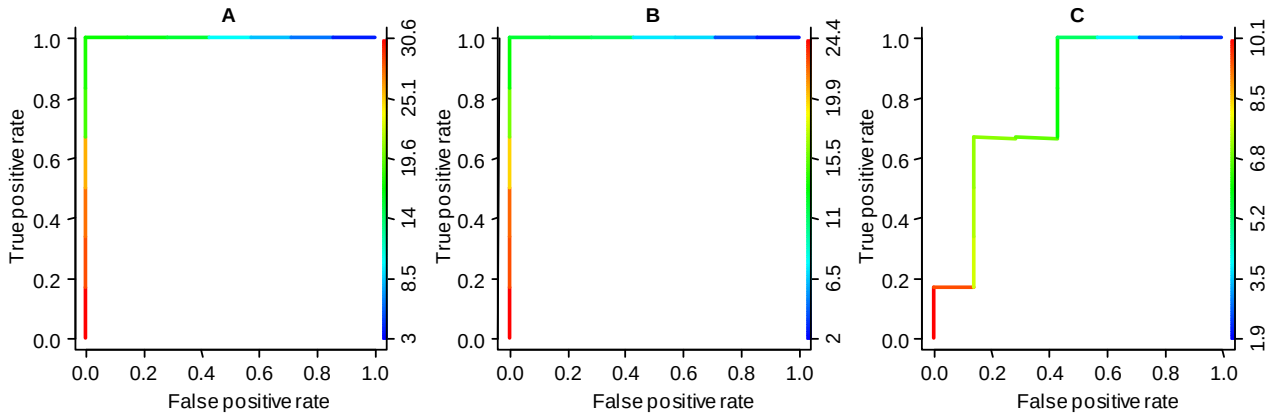

Figure 20. ROC analysis for thresholds calculation. Panel A: threshold for total delivered energy load to the respiratory system for VILI development 16.7 J/min, Specificity 100%, Sensibility 100%. Panel B: threshold for delivered dynamic transpulmonary energy load for VILI development 12.1 J/min, Specificity 100%, Sensibility 100%. Panel C: threshold for delivered energy load to the lung for VILI development 6.9 J/min, Specificity 86%, Sensibility 67%.

Estimation of delivered dynamic transpulmonary energy load threshold on tidal volume delivered at respiratory rate of 15 breaths/minute

Previously published data suggest that, in healthy piglets, ventilator-induced lung damage develops at 54 hours only when a strain greater than 1.5-2 is reached or overcome at a respiratory rate of 15 breaths/min.[1] We estimated the delivered dynamic transpulmonary energy load corresponding to this "threshold" from the 6 piglets' equations.

In our 6 piglets, average functional residual capacity was 246 ml and average weight 18.5 Kg. A strain of 1.5 corresponded to a delivered dynamic transpulmonary energy per breath of 0.57 J, corresponding to a delivered dynamic transpulmonary energy load of 8.6 J/min. A strain of 2 corresponded to a delivered dynamic transpulmonary energy per breath of 1.02 J, corresponding to a delivered dynamic transpulmonary energy load of 15.3 J/min.

Table 1. Clinical variables at the end of the study in piglets ventilated with a delivered dynamic transpulmonary energy load per minute below and above lethal threshold

		< 12.1 J/min n=9	**≥ 12.1 J/min** n=6	**P-value**
Weight (kg)		21±2	20±2	0.47
V_T	**(ml)**	783±67	817±88	0.46
	(ml/kg)	37±2	40±1	0.02
Strain (V_T/FRC)		2.99±0.59	10±8.41	0.23
V_T/tissue (ml/g)		2.03±0.3	1.41±0.43	0.02
Study duration (hour)		56.2±5.5	29.4±14.2	<0.01
Peak pressure (cmH_2O)		40±10	63±12	<0.01
Plateau pressure (cmH_2O)		26±7	41±12	0.18
Transpulmonary pressure (cmH_2O)		18±5	29±6	<0.01
PaO_2/FiO_2		470±77	282±182	0.09
pH		7.45±0.09	7.39±0.18	0.53
$PaCO_2$ (mmHg)		36.2±21.9	18.0±8.6	0.15
Respiratory System Elastance (cmH_2O/l)		32±11	42±12	0.18
Lung Elastance (cmH_2O/l)		25±10	39±10	0.02
Chest Wall Elastance (cmH_2O/l)		7±4	5±5	0.52
Mean Arterial Pressure (mmHg)		88±9	67±26	0.04
Heart Rate (bpm)		83±21	118±38	0.11
Lactates (mEq/l)		0.6±0.3	3.4±3.8	0.10
SvO_2 (%)		70±12	50±10	0.01
Fluid balance (ml)		-897±1284	1441±1233	0.01
Total lung volume (ml)		658±46	810±153	0.10
Total lung tissue (g)		387±31	614±152	<0.01
Well inflated tissue (%)		27±17	14±21	0.10
Poorly inflated tissue (%)		61±14	35±21	0.02
Not-inflated tissue (%)		12±8	51±36	0.07
Recruitment (%)		6±6	39±31	0.05
Inhomogeneity extent (%)		10±3	14±9	0.94
Autoptic lung weight (g)		313±165	496±125	0.02
Wet to dry ratio		5.7±1.4	6.9±1.1	0.18

Data are presented as mean ± standard deviation. The two groups were compared with two-tailed Wilcoxon Signed-Ranks Test. CT scan was not available in two piglets (both ventilated with a delivered dynamic transpulmonary energy

load per minute <16.7 J/min), so CT scan data were computed on 13 piglets. Fluid balance does not include drugs. Wet to dry ratio was computed in 11 piglets (respectively 6 and 5 in groups ventilated with low and high energy load).

Table 2. Energy load at the end of the study in piglets ventilated with delivered dynamic transpulmonary energy load below and above the threshold

	< 12.1 J/min n=9	**≥ 12.1 J/min** n=6	**P-value**
Delivered dynamic TP energy per breath (J)	1.2±0.3	2.5±0.3	<0.001
Average Inspiratory Flow (l/s)	0.25±0.11	0.50±0.10	<0.001
Delivered dynamic TP energy per minute (J/min)	7.6±4.2	33.5±7.7	<0.001

Data are presented as mean ± standard deviation. The two groups were compared with two-tailed Wilcoxon Signed-Ranks Test.

Relationships between increase of stress relaxation (P_1-P_2 cmH_2O) and VILI development

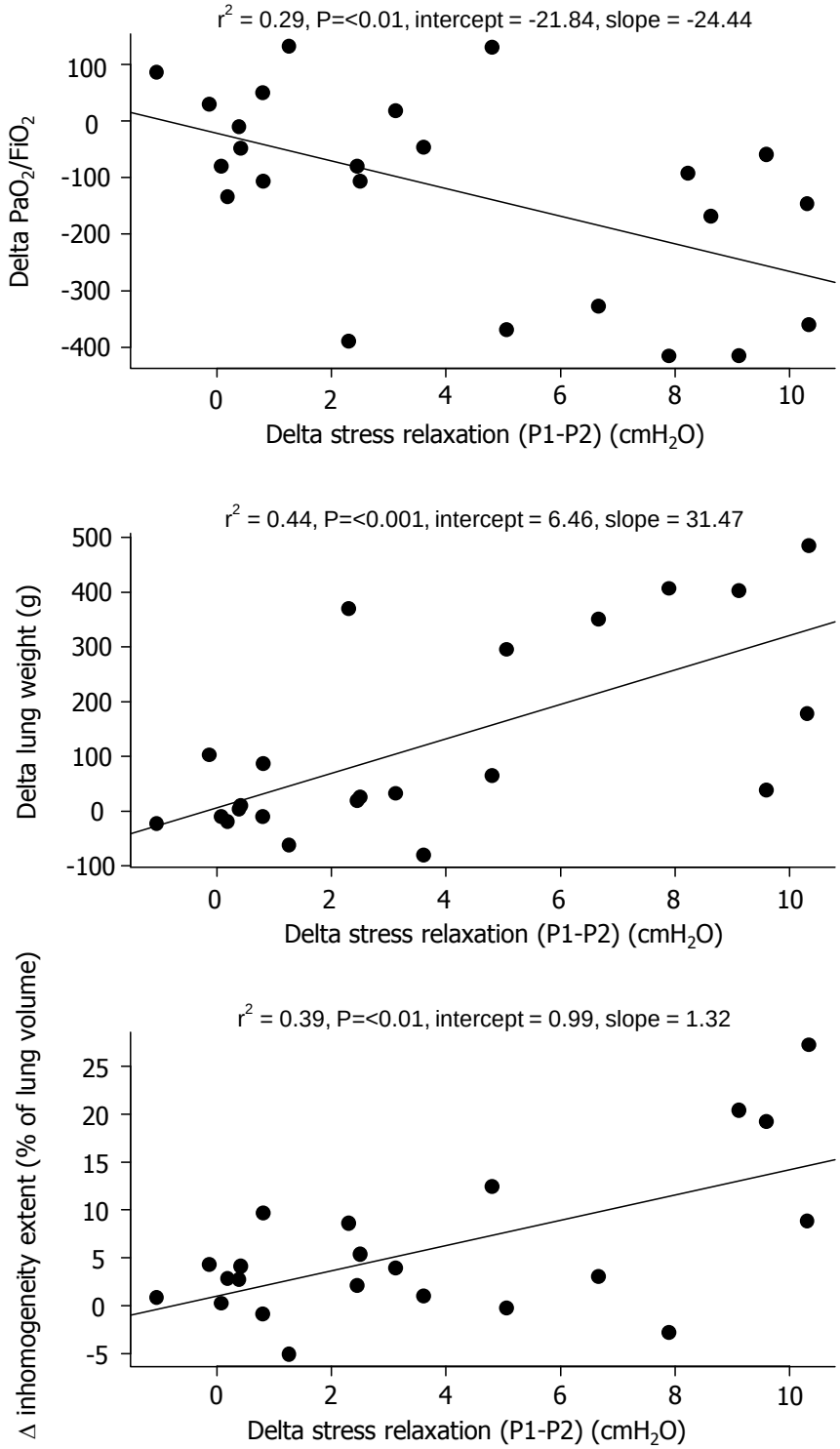

Figure 21: Relationships between increase of stress relaxation (P1-P2 cmH_2O) and VILI development

Histology

Histological analysis was available in 13 piglets: 9 from the main experiments (3 ventilated at 15 breaths/min, 2 ventilated at 12 breaths/min, 1 ventilated at 9 breaths/min and 3 ventilated at 6 breaths/min) and 4 from the confirmatory experiments (RR 35 breaths/min). For each of the histological parameters considered we computed a median value in each piglet (8 samples/piglet) (Table 7 and Figure 22).

Table 7: Histology

	No ventilator-induced lung edema (6 piglets)	**Ventilator induced lung edema (7 piglets)**	**P-value**
Hyaline membranes	0.69 [0.53-0.84]	1.75 [1.28-1.76]	0.03
Ruptured alveoli	0.50 [0.36-0.59]	0.37 [0.11-0.81]	0.89
Interstitial infiltrate	1.94 [1.31-2.09]	1.75 [1.61-2.19]	0.89
Infiltrate intensity	1.60 [1.30-1.75]	1.50 [1.41-1.56]	1.00
Intra-alveolar infiltrate	0.00 [0.00-0.19]	0.50 [0.34-0.77]	0.08
Red blood cells leakage	1.50 [1.22-1.88]	1.00 [0.81-1.00]	0.01

Piglets were divided according to the presence/absence of ventilator-induced lung edema. Data are presented as median [interquartile range] and compared with Wilcoxon test.

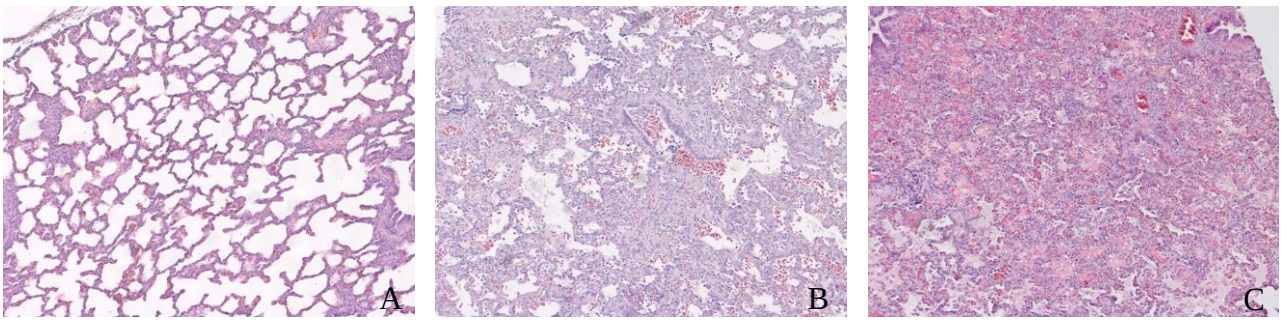

Figure 22: Photomicrographs of lung sections stained with haematoxylin-eosin showing the effect of delivered dynamic energy load below (A) and above (B, C) the threshold. At high delivered dynamic energy load lung injury is evident and characterized by hyaline membranes, capillary congestion and hemorrhaging, inter- and intra-alveolar infiltratum containing red and white blood cells, alveoli thickening and collapse, deposition of basophilic material on alveoli walls, leading to lung structure disruption. Original magnification: 10x.

Supplemental references

1. Protti A, Cressoni M, Santini A, Langer T, Mietto C, Febres D, Chierichetti M, Coppola S, Conte G, Gatti S, Leopardi O, Masson S, Lombardi L, Lazzerini M, Rampoldi E, Cadringher P, Gattinoni L: Lung stress and strain during mechanical ventilation: any safe threshold? Am J Respir Crit Care Med 2011; 183:1354–62

2. Cressoni M, Chiurazzi C, Gotti M, Amini M, Brioni M, Algieri I, Cammaroto A, Rovati C, Massari D, Castiglione CB di, Nikolla K, Montaruli C, Lazzerini M, Dondossola D, Colombo A, Gatti S, Valerio V, Gagliano N, Carlesso E, Gattinoni L: Lung Inhomogeneities and Time Course of Ventilator-induced Mechanical Injuries. Anesthesiology 2015doi:10.1097/ALN.0000000000000727

3. Weibel ER, Sapoval B, Filoche M: Design of peripheral airways for efficient gas exchange. Respir. Physiol. Neurobiol. 2005; 148:3–21

4. Cressoni M, Cadringher P, Chiurazzi C, Amini M, Gallazzi E, Marino A, Brioni M, Carlesso E, Chiumello D, Quintel M, Bugedo G, Gattinoni L: Lung inhomogeneity in patients with acute respiratory distress syndrome. Am. J. Respir. Crit. Care Med. 2014; 189:149–58